Evidence for O_{2p} Hole-Driven Conductivity in $La_{1-x}Sr_xMnO_3$ ($0 \leq x \leq 0.7$) and $La_{0.7}Sr_{0.3}MnO_z$ Thin Films

H. L. Ju, H.-C. Sohn, and Kannan M. Krishnan*

Materials Sciences Division, Lawrence Berkeley National Laboratory, 1 Cyclotron Road, Berkeley, California 94720

(Received 2 December 1996)

Oxygen K-edge electron-energy-loss spectra have been measured for $La_{1-x}Sr_xMnO_3$ ($0 \leq x \leq 0.7$) and $La_{0.7}Sr_{0.3}MnO_z$ thin films as a function of x and z. The spectra show a prepeak at the Fermi level, corresponding to transitions to empty states in the O_{2p} band, at the threshold of the K edge around 529 eV. This prepeak systematically increases with an increase in conductivity through divalent doping (x) or oxygen content (z). This confirms that these materials are charge-transfer-type oxides with carriers having significant oxygen $2p$ hole character. We argue that, the double exchange mechanism has to include the role of oxygen hole density to satisfactorily describe their transport properties. [S0031-9007(97)04413-X]

PACS numbers: 71.38.+i, 72.15.Gd, 75.30.Kz

Manganites with the general formula $R_{1-x}A_xMnO_3$ (R = La, Pr, Nd, Sm: A = Ca, Sr, Ba, Pb) exhibiting "colossal" magnetoresistance (CMR) have generated much recent interest [1,2]. The parent $RMnO_3$ (Mn^{3+}; $t_{2g}{}^3e_g^1$) is a magnetic insulator, but $R_{1-x}A_xMnO_3$ transforms into a metallic ferromagnet upon doping ($0.2 \leq x \leq 0.5$) [3,4] and exhibits CMR near its ferromagnetic transition temperature (T_C) [3]. The coexistence of ferromagnetism and metallic behavior is traditionally explained within the framework of "*double exchange*" (DE) [5,6], where the transfer integral for an electron is proportional to $\cos(\theta_{ij}/2)$, and θ_{ij} is the angle between two ionic spins. The conductivity is a maximum when the on-site Hund exchange energy is a minimum and hence ferromagnetism is coupled with metallic behavior. Thus the DE mechanism qualitatively explains why these manganites become metallic below T_C (well-aligned spins) and insulating above T_C (randomly aligned spins), and show large magnetoresistance values due to field induced spin alignment.

Insulating compounds arising from strong correlation between d electrons can be categorized into either Mott-Hubbard or charge-transfer materials [7]. In the former, the insulating gap (Mott-Hubbard gap U) is between the d-electron states (upper Hubbard and lower Hubbard bands), whereas in the latter, the gap (charge transfer gap Δ) is between the oxygen p-like state and the unoccupied d-like upper Hubbard band. In this simple model, doping induces holes in the oxygen sites (charge-transfer-type) or in the lower Hubbard band (Mott-Hubbard-type) [7,8]. Thus the DE mechanism implicitly assumes a Mott-Hubbard-type insulator [9] requiring Mn^{3+}/Mn^{4+} mixtures and contradicts the fact that $RMnO_3$ is known [10,11] to be a charge-transfer insulator. Hence, the nature of the insulating gap and the charge carriers in CMR materials needs to be investigated in detail.

Established techniques for the determination of the electronic structure of such materials, such as x-ray photoelectron (XPS) and x-ray absorption (XAS) spectroscopies, are only surface sensitive with probing depths of 10–50 Å. To be effective, these techniques require that the surfaces prepared have electronic structures representative of the bulk. This is particularly difficult to achieve for these perovskite manganites since their surfaces are chemically unstable [11]. Electron-energy-loss spectra (EELS) in a transmission electron microscope (TEM) are ideally suited for such measurements—the measurement is carried out in transmission through 500–800 Å thick samples, and its potential for determining the electronic structure of perovskites was demonstrated in studies of high T_C cuprate superconductors [12]. In this Letter we report our results of EELS measurements of the O_K edge (excitation of O_{1s} electrons into empty p-like states following dipole selection rules) in $La_{1-x}Sr_xMnO_3$ ($0 \leq x \leq 0.7$) and $La_{0.7}Sr_{0.3}MnO_z$ films as a fucntion of x and z. Indeed, in a systematic study of well-characterized, epitaxially grown, thin films we have found a prepeak (O_{2p} holes) at the Fermi level, the intensity of which correlates well with the electrical conductivity of the films over the entire range of divalent-dopant or oxygen content.

Manganite films of nominal composition $La_{1-x}Sr_xMnO_3$ ($0 \leq x \leq 0.7$) and $La_{0.7}Sr_{0.3}MnO_z$ were grown epitaxially on (100) $LaAlO_3$ substrates by a polymeric sol-gel technique [13]. $La_{1-x}Sr_xMnO_3$ films were finally annealed at 700 °C for 1 h in air. The $La_{0.7}Sr_{0.3}MnO_z$ films were first annealed at 900 °C/O_2/1 h. Twenty such as-prepared films, showing identical resistivity and field response, were subsequently vacuum (10^{-6} Torr) annealed at different temperatures (450, 500, 550, and 650 °C) for 2 h to systematically vary their oxygen stoichiometry. All films were characterized by x-ray diffraction before and after anneal to ensure that they remained single phase even after annealing at 650 °C. Relative oxygen content of the films, measured by energy dispersive x-ray spectroscopy (EDXS) using experimentally measured k factors [14], show that the films annealed at 550 °C have ~3% less oxygen than the as-prepared films. Conventional four-point dc resistivities

 0031-9007/97/79(17)/3230(4)$10.00

were measured using a home-built probe in a field of up to 1 T. EELS data was obtained using a Philips CM200 microscope equipped with a field-emission source and a Gatan imaging filter. Spectra were obtained in image mode with a probe convergence angle of 4.0 mrad and 1 eV energy resolution.

Figure 1(a) illustrates the temperature dependence of the resistivity for $La_{1-x}Sr_xMnO_3$ films. Low doped ($x \leq 0.1$) films show insulating behavior over the entire temperature range. With increasing doping, resistivity decreases—for $x = 0.2$, a typical metal-insulator transition [15] is observed at ~260 K; $x = 0.3$ shows metallic behavior and, in addition, has the lowest resistivity. The resistivity increases again at higher doping ($x \geq 0.4$), and for $x > 0.6$ the films show insulating behavior. Figure 1(b) shows the region near the threshold of the O_K edge in the EELS spectrum of $La_{1-x}Sr_xMnO_3$ films and the $LaAlO_3$ substrate. The XPS binding energy, $E_b = 529$ eV [11], which indicates the energy of the O_{1s} level with respect to the Fermi energy, is also marked by a narrow band. In EELS, fine structures of the O_K edge can be interpreted in terms of transition processes governed by the dipole selection rule ($\Delta l = \pm 1$) [16]. Thus, the first feature, the prepeak around 529 eV, is attributed to transitions from O_{1s} to unoccupied states in the O_{2p} band. For quantitative comparison, the prepeak intensities above a linear background were normalized with the main peak intensity at ~535 eV. These normalized values are 7.7 for $x = 0$, 9.5 for $x = 0.3$, and 8.5 for $x = 0.4$. For $LaAlO_3$ no prepeak is observed, and the sharp rise in spectral intensity marking the onset of the edge ~3 eV above E_F (i.e., at ~532 eV) is attributed to La_{5d} and La_{4f} states hybridized with O_{2p} states. The absence of the prepeak in $LaAlO_3$, an ionic insulator with completely filled O_{2p} states, and its appearance in the $La_{1-x}Sr_xMnO_3$ series is a reflection of the presence in the latter of holes on oxygen sites leading to p-type conductivity. Moreover, the prepeak intensity in $La_{1-x}Sr_xMnO_3$ varies systematically with the conductivity of the films and not with their divalent-dopant content. In addition, neither of O_K edge threshold peaks (~532 eV) nor the Mn $L_{3,2}$ (spin-orbit split $2p^{3/2}$ and $2p^{1/2}$ to unoccupied $3d$) transitions (the latter not shown) present any discernible change in intensities with divalent doping and/or conductivity of the films.

Of central importance to this interpretation is the following question: On which site do the electrons/holes reside when substitutions are made? XAS studies of early transition metals (Ti, V) in three series of oxides [17] as a function of substitution indicated that extra electrons/holes are located primarily at the $3d$ metal site, while in late $3d$ transition metal (Ni) oxides, holes induced by doping have predominantly oxygen $2p$ character [18]. The crossover behavior of transition metal systems in the middle of the row (Fe, Mn) are not easily predictable with the added possibility of extra charges having mixed transition metal $3d$-oxygen $2p$ character [19]. However, studies [20] of oxygen K-edge absorption spectra of $La_{2-x}Sr_xCuO_{4+d}$ reveal two distinct pre-edge features (at 530 and 528 eV, respectively) which evolve systematically with Sr concentration ($0 < x < 0.15$). The peak at 530 eV, corresponding to transitions into the upper Hubbard band, is most intense in the insulating state and decreases with Sr doping. The second peak at 528 eV, attributed to transitions into the charge-transfer band (extra holes on oxygen sites), grows in intensity and shifts to lower energy with Sr addition. The pre-edge features observed [Fig. 1(b)] appear to fit this description but with significant differences. The divalent-dopant concentration in our experiments is much higher, and, if the above trend with Sr doping continued to be valid, it would be expected that the pre-edge feature in our measurements can be

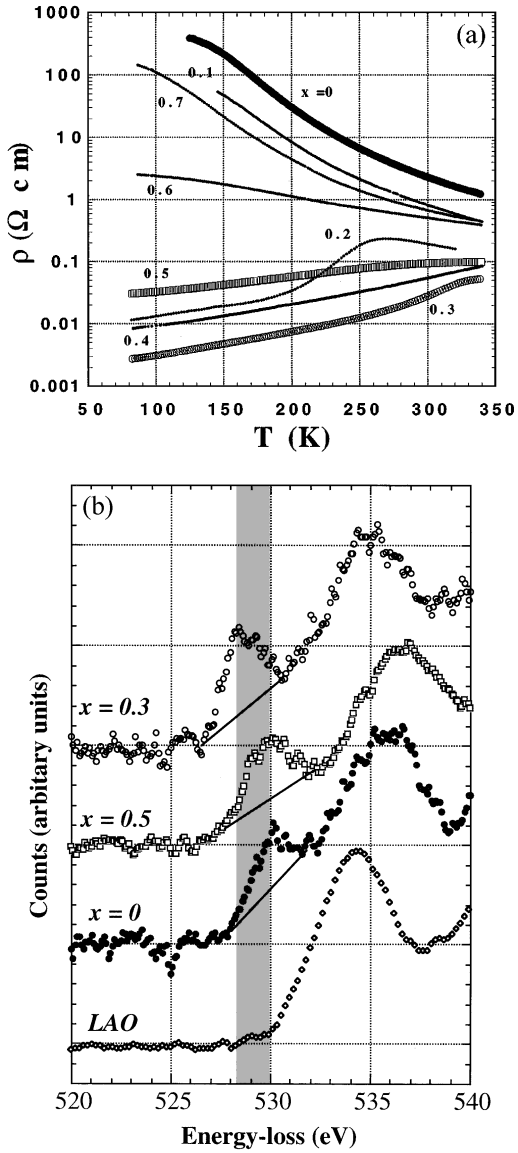

FIG. 1. (a) Temperature dependence of the resistivity of the $La_{1-x}Sr_xMnO_3$ films in the composition range $0 \leq x \leq 0.7$. (b) Oxygen K-edge spectra of $La_{1-x}Sr_xMnO_3$ ($x = 0$, 0.3, 0.5) and $LaAlO_3$. The small shifts in the energies of the peaks is due to drift in the high voltage offsets.

attributed to transition into the charge-transfer band. In any case, the key result is that the overall intensity of the pre-edge feature increases with the conductivity of the films and not with the divalent doping concentration.

It is believed [21] that the magnetotransport properties of these films are strongly dependent on the oxygen stoichiometry. In fact, improper control of the oxygen content in the films can also contribute noticeably to the prepeak intensity. Moreover, the hole peak intensity is a function of Sr content, oxygen content, and Mn valence. In the first set of experiments [Figs. 1(a) and 1(b)], Mn valence is constant within the resolution of our measurements. However, the oxygen content can also be expected to vary with Sr content. In order to sort this further, we have carried out a second set of experiments, i.e., further fixed Sr content and systematically varied oxygen content by high-temperature vacuum annealing over a range of temperatures, and established a correlation between resistivity, oxygen stoichiometry, and the O_{2p} hole density. The temperature dependence of the resistivity for $La_{0.7}Sr_{0.3}MnO_z$ is shown in Fig. 2(a). Though the as-prepared films show a metallic resistivity for the entire temperature range investigated, the low temperature (450, 500 °C) vacuum annealed samples show metal-insulator transitions, and the high temperature (550, 650 °C) vacuum annealed samples show insulating behavior.

Figure 2(b) shows the O_K edge in EELS of as-prepared and $La_{0.7}Sr_{0.3}MnO_z$ films vacuum annealed at 550 °C. As-prepared $La_{0.7}Sr_{0.3}MnO_z$ shows a large prepeak in the O_K edge which disappears when the film is vacuum annealed at 550 °C. Once again, the prepeak intensity correlates well with the conductivity confirming the significant role of O_{2p} hole density in determining the magnitude of the resistivity.

Over the range of $La_{1-x}Sr_xMnO_3$ and $La_{0.7}Sr_{0.3}MnO_z$ samples studied, we have observed a significant prepeak at the Fermi level in the O_K edge in EELS, with intensity closely related to the conductivity of the films. The absence of this O_K prepeak in $LaAlO_3$ and its presence in these compounds suggest that the latter are charge transfer type oxides. Specifically, doping the parent $LaMnO_3$ with divalent Sr generates unoccupied states in the O_{2p} band, and vacuum annealing of $La_{0.7}Sr_{0.3}MnO_z$ to systematically control oxygen stoichiometry reduces O_{2p} hole density. Divalent doping or change in the oxidation state could also generate Mn^{4+} (Mn holes), but within the sensitivity of our EELS measurements the Mn $L_{3,2}$ transitions show no discernible change in peak shape or in intensity. These measurements are in contrast with the conventional DE mechanism, where doping is assumed to induce holes on Mn sites (Mn^{4+}), and the interaction between Mn^{3+} and Mn^{4+} drives the ferromagnetic behavior and enhanced conductivity. The O_{2p} hole density, which increases with doping of $LaMnO_3$, has a clear correlation with resistivity, i.e., the larger the O_{2p} hole density, the smaller the resistivity. This observation implies that the conductivity in these materials is hole driven and

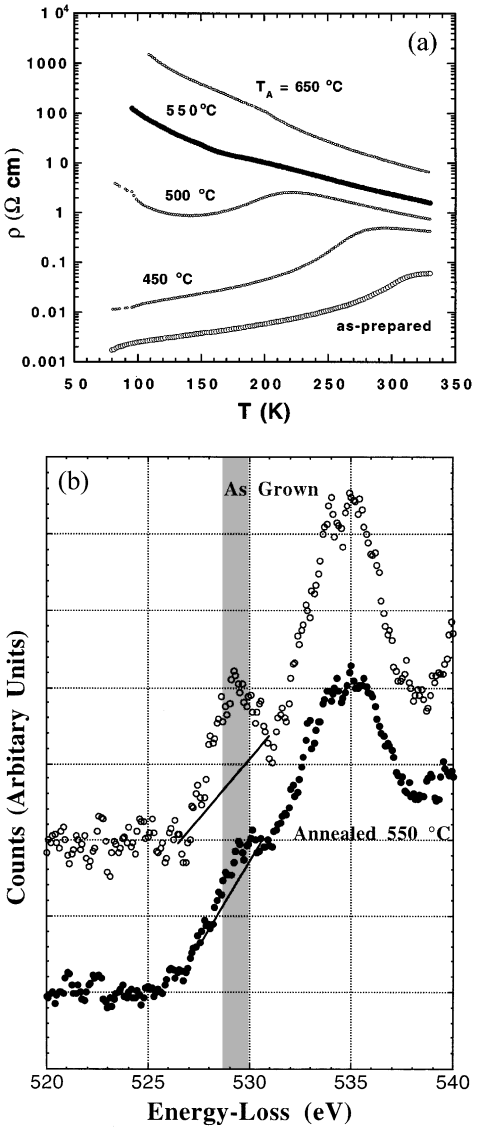

FIG. 2. (a) Temperature dependence of the resistivity of the $La_{0.7}Sr_{0.3}MnO_z$ films which were annealed in a vacuum of 10^{-6} Torr for 2 h at 450, 500, 550, and 650 °C. (b) Oxygen K-edge spectra of $La_{0.7}Sr_{0.3}MnO_z$ as-prepared and vacuum annealed film at 550 °C.

that these holes, having predominantly O_{2p} hole character, contribute significantly to the conduction mechanism, including magnetoresistance, in these materials.

Even though our EELS measurements of $La_{1-x}Sr_xMnO_3$ and $La_{0.7}Sr_{0.3}MnO_z$ show a pre-O_K peak with intensity related to the electrical conductivity, this intensity does not vary linearly with the divalent-dopant concentration, i.e., shows a maximum value for $x = 0.3$. Since the charge transfer model predicts that more doping introduces more holes on oxygen sites, this may indicate a simultaneous change in electronic structure with doping. As is well known in ABO_3 (A = rare earth, $B = 3d$ transition metal) [8,22], the B-O-B or Mn-O-Mn bond angle, Θ has significant effects on electronic bandwidth and magnetic exchange interaction in perovskite

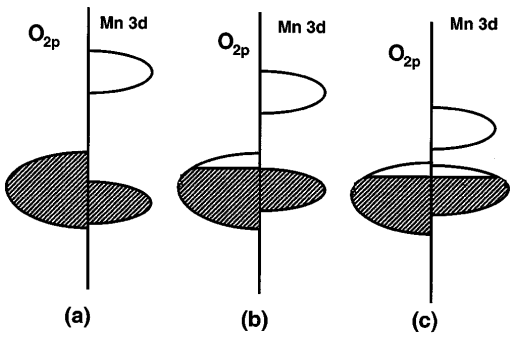

FIG. 3. Proposed band evolution of $La_{1-x}Sr_xMnO_3$ as a function of x. (a) Low doped region ($x < 0.2$), (b) intermediate doped region ($\sim 0.2 < x < 0.4$), (c) high doped region ($\sim 0.4 < x < 0.5$).

structures. For undoped $LaMnO_3$, $\Theta < 180°$ and leads to orthorhombic distortion, but with divalent doping the Mn-O distance decreases and the structure approaches cubic for $x = 0.3$ with $\Theta \sim 180°$. Hence, doping with Sr^{2+} causes Θ to approach 180° with an accompanying increase in bandwidth. In addition to the increase in bandwidth, doping may also induce a decrease in electron correlation energy, thus reducing the Mott-Hubbard gap (U). As the bandwidth increases and U decreases with increasing divalent doping, upper and lower Hubbard bands may overlap, giving rise to metallic conductivity with the charge carriers taking on both electron and hole character. A schematic band diagram illustrating these ideas is shown in Fig. 3.

In summary, we have made systematic measurements of the O_K edge in EELS spectra of $La_{1-x}Sr_xMnO_3$ and $La_{0.7}Sr_{0.3}MnO_z$ thin films. We have observed a prepeak at the Fermi level, corresponding to the unoccupied density of states at the oxygen site. This prepeak intensity increases with an increase in conductivity, both with doping and variation of oxygen stoichiometry. This suggests that the charge carriers responsible for the conduction mechanism in these manganese oxides have significant oxygen $2p$ hole character. The double-exchange mechanism (DEM) implicitly assumes a Mott-Hubbard-type material. Millis *et al.* [6] argued that, in addition to double exchange, lattice distortions (polaron) effects need to be incorporated into the description of the resistivity of these materials. However, our data shows that these manganite perovskites are charge-transfer-type oxides, and we argue that DEM without considering the oxygen hole density (and to a much smaller extent their hybridization effects) is not complete. These observations provide new insight into the transport mechanism in these manganite perovskites.

We thank A. R. Modak and C. Nelson for experimental assistance, and J. B. Torrance for helpful discussions. This work was supported by the Director, Office of Energy Research, Office of Basic Energy Sciences, Materials Sciences Division of the U.S. Department of Energy, under Contract No. DE-AC03-76SF00098.

*To whom all future correspondence should be addressed.

[1] R. von Helmolt, J. Wecker, B. Holzapfel, L. Schultz, and K. Samwer, Phys. Rev. Lett. **71**, 2331 (1993); K. Chahara, T. Ohno, M. Kasai, and Y. Kozono, Appl. Phys. Lett. **63**, 1990 (1993).
[2] R. H. Heffner, L. P. Le, M. F. Hundley, J. J. Neumeier, G. M. Luke, K. Kojima, B. Nachumi, Y. J. Uemura, D. E. MacLaughlin, and S-W. Cheong, Phys. Rev. Lett. **77**, 1869 (1996).
[3] A. Urushibara, Y. Moritomo, T. Arima, A. Asamitsu, G. Kito, and Y. Tokura, Phys. Rev. B **51**, 14 103 (1995).
[4] G. H. Jonker and J. H. Van Santen, Physica (Utrecht) **16**, 337 (1950).
[5] P. G. de Gennes, Phys. Rev. **118**, 141 (1960).
[6] A. J. Millis, P. B. Littlewood, and B. I. Shraiman, Phys. Rev. Lett. **74**, 5144 (1995).
[7] G. A. Zaanen, G. A. Sawatzky, and J. W. Allen, Phys. Rev. Lett. **55**, 418 (1985).
[8] J. B. Torrance, P. Lacorre, A. I. Nazzal, E. J. Ansaldo, and C. Niedermayer, Phys. Rev. B **45**, 8209 (1992).
[9] T. Tokura, A. Urushibara, Y. Moritomo, A. Asamitsu, Y. Tomioka, T. Arima, and G. Kido, Mater. Sci. Eng. B **31**, 187 (1995).
[10] J. B. Torrance, Physica (Amsterdam) **182C**, 351 (1991).
[11] T. Saitoh, A. E. Bocquet, T. Mizokawa, H. Namatame, A. Fujimori, M. Abbate, Y. Takeda, and M. Takano, Phys. Rev. B **51**, 13 942 (1995).
[12] N. Nücker, J. Fink, J. C. Fuggle, P. J. Durham, and W. M. Temmerman, Phys. Rev. B **37**, 5158 (1988).
[13] Kannan M. Krishnan, A. R. Modak, H. L. Ju, and P. Bamdaru, Ceram. Microstruct. (to be published).
[14] Kannan M. Krishnan and C. J. Echer, *Analytical Electron Microscopy*, edited by D. C. Joy (San Francisco Press, San Francisco, 1987).
[15] A. Gupta, T. R. MaGuire, P. R. Duncombe, M. Rupp, J. Z. Sun, W. J. Gallagher, and Gang Xiao, Appl. Phys. Lett. **67**, 3494 (1995).
[16] R. F. Egerton, *EELS in the Electron Microscope* (Plenum, New York, 1986).
[17] M. Abbate, F. M. F. de Groot, J. C. Fuggle, A. Fujimori, Y. Tokura, Y. Fujishima, O. Strebel, M. Domke, J. van Elp, B. T. Thole, G. A. Sawatzky, M. Sacchi, and N. Tsuda, Phys. Rev. B **44**, 5419 (1991).
[18] P. Kuiper, G. Kruizinga, J. Ghijsen, G. A. Sawatzky, and H. Verweij, Phys. Rev. Lett. **62**, 221 (1989); P. Kuiper, J. van Elp, G. A. Sawatzky, A. Fujimori, S. Hosoya, and D. M. de Leeuw, Phys. Rev. B **44**, 4570 (1991).
[19] M. Abbate, F. M. F. de Groot, J. C. Fuggle, A. Fujimori, O. Strebel, F. Lopez, M. Domke, G. Kaindl, G. A. Sawatzky, M. Takano, Y. Takeda, H. Eisaki, and S. Uchida, Phys. Rev. B **46**, 4511 (1992).
[20] C. T. Chen, F. Sette, Y. Ma, M. S. Hybertsen, E. B. Stechel, W. M. C. Foulkes, M. Schluter, S-W. Cheng, A. S. Cooper, L. W. Rupp, Jr., B. Batlogg, Y. L. Soo, Z. H. Ming, A. Krol, and Y. H. Kao, Phys. Rev. Lett. **66**, 104 (1991).
[21] M. Verelst, N. Rangavittal, C. N. R. Rao, and A. Rousset, J. Solid State Chem. **104**, 74 (1993).
[22] C. Eylem, H. L. Ju, B. Eichhorn, and R. L. Greene, J. Solid State Chem. **114**, 164 (1995).